Instabilities of rotational flows in azimuthal magnetic fields of arbitrary radial dependence

2014 Fluid Dyn. Res. 46 031403

(http://iopscience.iop.org/1873-7005/46/3/031403)

IOP Publishing | The Japan Society of Fluid Mechanics Fluid *Dynamics* Research

Fluid Dyn. Res. **46** (2014) 031403 (14pp) doi:10.1088/0169-5983/46/3/031403

Instabilities of rotational flows in azimuthal magnetic fields of arbitrary radial dependence

Oleg N Kirillov[1], **Frank Stefani**[1] **and Yasuhide Fukumoto**[2]

[1] Helmholtz-Zentrum Dresden-Rossendorf, PO Box 510119, D-01314 Dresden, Germany
[2] Institute of Mathematics for Industry, University of Kyushu, 744 Motooka, Nishi-ku, Fukuoka 819-0395, Japan

E-mail: o.kirillov@hzdr.de, f.stefani@hzdr.de and yasuhide@imi.kyushu-u.ac.jp

Received 9 July 2013, revised 16 November 2013
Accepted for publication 20 December 2013
Published 27 May 2014

Communicated by M Funakoshi

Abstract

Using the Wentzel–Kramers–Brillouin (WKB) approximation we perform a linear stability analysis for a rotational flow of a viscous and electrically conducting fluid in an external azimuthal magnetic field that has an arbitrary radial profile $B_\phi(R)$. In the inductionless approximation, we find the growth rate of the three-dimensional perturbation in a closed form and demonstrate in particular that it can be positive when the velocity profile is Keplerian and the magnetic field profile is slightly shallower than R^{-1}.

(Some figures may appear in colour only in the online journal)

1. Introduction

Recently, magnetorotational instability (MRI), discovered by Velikhov (1959) and Chandrasekhar (1960), has experienced a significant revival for its promise to explain the destabilization and turbulization of Keplerian discs and, consequently, the outward transport of angular momentum and the accretion of matter to a gravitating central body such as a black hole or a protostar (Balbus 2003). Complementary to the extensive numerical research with the main focus on astrophysical applications, there is also some activity to reproduce MRI in the liquid metal laboratory. To date, any clear identification of the standard version of MRI (SMRI), with an axial magnetic field being applied, has been hampered by the necessity to reach quite large magnetic Reynolds numbers (in the order of 10). Since liquid metals are

characterized by a very small magnetic Prandtl number Pm (the ratio of viscosity to magnetic diffusivity), this implies that the hydrodynamic Reynolds numbers must be in the order of millions, a number at which experimental Taylor–Couette flows are very hard to maintain stable due to the effects of axial boundaries.

It came, therefore, as a great surprise when Hollerbach and Rüdiger (2005) discovered an alternative version of MRI whose onset does not depend on the magnetic Reynolds number or the Lundquist number, such as SMRI, but only on the Reynolds number and the Hartmann number. This new MRI version relies on an appropriate combination of an axial and an azimuthal magnetic field, and has therefore been coined helical MRI (HMRI). Further, a non-axisymmetric version, the azimuthal MRI (AMRI), has been shown to become dominant for purely or strongly dominant azimuthal magnetic fields (Hollerbach *et al* 2010, Rüdiger *et al* 2013).

Whereas the scaling of HMRI (and AMRI) with the Reynolds and Hartmann numbers is quite attractive for experimental studies (Stefani *et al* 2006, 2009), a somewhat unattractive feature of these inductionless MRI versions had been identified by Liu *et al* (2006). It concerns the apparent failure of HMRI to work for comparably shallow rotation profiles, including the Keplerian profile that is the most relevant one for astrophysics. For the inductionless case, with $Pm = 0$, the authors had identified two limits for the steepness of the rotation profile, one for negative, the other one for positive Rossby number Ro, between which HMRI ceases to exist. Later, the significance of both limits was extended to the case of AMRI, and even to higher azimuthal wavenumbers (Kirillov and Stefani 2010, Kirillov *et al* 2012).

The relevance of the inductionless limit is not restricted to the academic case of liquid metal experiments. Small magnetic Prandtl numbers appear as well in the outer parts of accretion discs around black holes (Balbus and Henri 2008), in protoplanetary discs (Armitage 2011), and in the liquid metal cores of Earth-like planets (Petitdemange *et al* 2008). Given the dramatically different scaling laws of SMRI and HMRI/AMRI it is of great importance to determine the range of applicability of the latter.

In a recent letter (Kirillov and Stefani 2013) we have discussed a simple way of extending this range. We set out from the consideration that the current-free assumption for the azimuthal magnetic field, i.e. $B_\phi(R) \propto 1/R$, as it was assumed theoretically and imposed experimentally to date, has no particular astrophysical foundation. Quite in contrast, it is rather clear that B_ϕ in the disc may have a complicated spatial structure that is a function of the axial and radial dependences of conductivity and viscosity. This applies both to the case where an axial magnetic field B_z is externally applied, from which B_ϕ is then induced, as well as to the case $B_z = 0$ so that B_ϕ must be produced by some sort of dynamo (Herault *et al* 2011). An instructive illustration of the induction of a toroidal field from an applied poloidal field can be found in a recent paper by Colgate *et al* (2011) who had observed an eight-fold toroidal field gain in a liquid sodium Taylor–Couette flow with a magnetic Reynolds number (Rm) of 120. While certainly this mechanism cannot be transferred one-to-one to an accretion disc, which has no Ekman layers at its vertical edges, there are other vertical and radial variations of angular velocity and conductivity that would lead to similar induction effects. Without going into the details of magnetic field induction in various types of accretion discs, the idealized case of a current-free field, $B_\phi(R) \propto 1/R$, as produced by an assumed central axial current, is by far less likely than any shallower profile that is (at least partly) induced in the disc. Defining an appropriate magnetic Rossby number Rb for such general profiles $B_\phi(R)$, we showed that Keplerian profiles can easily be destabilized by HMRI or AMRI. We further showed that the upper and lower Liu limits in terms of Ro (Liu *et al* 2006) are just the endpoints of a continuous stability curve in the Rb–Ro plane.

Having thus evidenced that *formally* the inductionless versions of MRI, i.e. HMRI and AMRI, are well capable of destabilizing Keplerian, and even shallower, rotation profiles, one should notice a physical inconsistency of this argumentation. Certainly, any deviation of $B_\phi(R)$ from the current-free $1/R$ profile can only result from induction effects in the disc. Hence it would need some finite value of Rm, which is apparently in contrast with the original inductionless approximation.

As a follow-up of the letter (Kirillov and Stefani 2013), the present paper comprises a detailed derivation of the WKB stability analysis for arbitrary radial profiles of B_ϕ, quite in analogy to the procedure by Krueger *et al* (1966), Eckhardt and Yao (1995) and Friedlander and Vishik (1995). A further focus will then be on some strict results concerning the growth rate of the non-axisymmetric instability. Finally, using the Bilharz criterion we obtain the domain of AMRI of a Keplerian flow both in the inductionless case corresponding to the vanishing magnetic Reynolds number and in the case of finite Rm.

2. Mathematical setting

2.1. Basic equations and the base state

The standard set of nonlinear equations of dissipative incompressible magnetohydrodynamics (MHD) consists of the Navier–Stokes equation for the fluid velocity $\mathbf{u}$ and the induction equation for the magnetic field $\mathbf{B}$

$$\begin{aligned} &\frac{\partial \mathbf{u}}{\partial t} + \mathbf{u}\cdot\nabla\mathbf{u} - \frac{1}{\mu_0\rho}\mathbf{B}\cdot\nabla\mathbf{B} + \frac{1}{\rho}\nabla P - \nu\nabla^2\mathbf{u} = 0, \\ &\frac{\partial \mathbf{B}}{\partial t} + \mathbf{u}\cdot\nabla\mathbf{B} - \mathbf{B}\cdot\nabla\mathbf{u} - \eta\nabla^2\mathbf{B} = 0, \end{aligned} \tag{1}$$

where $P = p + \frac{\mathbf{B}^2}{2\mu_0}$ is the total pressure, p is the hydrodynamic pressure, $\rho = \text{const}$ the density, $\nu = \text{const}$ the kinematic viscosity, $\eta = (\mu_0\sigma)^{-1}$ the magnetic diffusivity, $\sigma = \text{const}$ the conductivity of the fluid and μ_0 the magnetic permeability of free space. Additionally, the mass continuity equation for incompressible flows and the solenoidal condition for the magnetic induction yield

$$\nabla\cdot\mathbf{u} = 0, \quad \nabla\cdot\mathbf{B} = 0. \tag{2}$$

Introducing cylindrical coordinates (R, ϕ, z), we consider the stability of a steady-state background liquid flow characterized by the angular velocity profile $\Omega(R)$ exposed to an azimuthal background magnetic field

$$\mathbf{u}_0(R) = R\,\Omega(R)\,\mathbf{e}_\phi, \quad p = p_0(R), \quad \mathbf{B}_0(R) = B_\phi^0(R)\mathbf{e}_\phi. \tag{3}$$

Note that if the azimuthal component is produced by a central axial current I, then

$$B_\phi^0(R) = \frac{\mu_0 I}{2\pi R}. \tag{4}$$

In case that it is produced by a homogeneous current in a cylindrical column of radius R_0, which is relevant for the onset of the Tayler instability (Seilmayer *et al* 2012), it would read as follows:

$$B_\phi^0(R) = \frac{\mu_0 I R}{2\pi R_0^2}. \tag{5}$$

The centrifugal acceleration of the background flow (3) is compensated by the pressure gradient

$$R\Omega^2 = \frac{1}{\rho}\frac{\partial p_0}{\partial R}. \tag{6}$$

An appropriate quantitative measure of the hydrodynamic shear is given by the *hydrodynamic Rossby number* (Ro) which we define by means of the relation

$$Ro = \frac{R}{2\Omega}\frac{\partial \Omega}{\partial R}. \tag{7}$$

With this definition, the solid body rotation corresponding to $\Omega(R) = \text{const}$ gives $Ro = 0$, the Keplerian rotation with $\Omega(R) \propto R^{-3/2}$ gives $Ro = -3/4$, whereas the velocity profile $\Omega(R) \propto R^{-2}$ leads to $Ro = -1$.

Similarly, we introduce the *magnetic Rossby number* (Rb) as

$$Rb = \frac{R}{2(B_\phi^0/R)}\frac{\partial (B_\phi^0/R)}{\partial R}. \tag{8}$$

Hence, $Rb = 0$ corresponds to the linear dependence of the magnetic field on the radius, $B_\phi^0(R) \propto R$, and $Rb = -1$ to the radial dependence given by equation (4).

2.2. Linearization with respect to non-axisymmetric perturbations

To describe natural oscillations in the neighborhood of the magnetized rotational flow we linearize equations (1) subject to the constraints (2) in the vicinity of the stationary solution (3) assuming general perturbations $\mathbf{u} = \mathbf{u}_0 + \mathbf{u}'$, $p = p_0 + p'$ and $\mathbf{B} = \mathbf{B}_0 + \mathbf{B}'$ and leaving only the terms of first order with respect to the primed quantities

$$\begin{gathered}\partial_t \mathbf{u}' + \mathbf{u}_0\cdot\nabla\mathbf{u}' + \mathbf{u}'\cdot\nabla\mathbf{u}_0 - \frac{1}{\rho\mu_0}\left(\mathbf{B}_0\cdot\nabla\mathbf{B}' + \mathbf{B}'\cdot\nabla\mathbf{B}_0\right) = \nu\nabla^2\mathbf{u}' - \frac{1}{\rho}\nabla p' - \frac{1}{\rho\mu_0}\nabla(\mathbf{B}_0\cdot\mathbf{B}'),\\ \partial_t \mathbf{B}' + \mathbf{u}_0\cdot\nabla\mathbf{B}' + \mathbf{u}'\cdot\nabla\mathbf{B}_0 - \mathbf{B}_0\cdot\nabla\mathbf{u}' - \mathbf{B}'\cdot\nabla\mathbf{u}_0 = \eta\nabla^2\mathbf{B}'.\end{gathered} \tag{9}$$

Here, the perturbations fulfill the constraints

$$\nabla\cdot\mathbf{u}' = 0, \quad \nabla\cdot\mathbf{B}' = 0. \tag{10}$$

With the gradients of the background fields represented by the 3×3 matrices

$$\begin{gathered}\mathcal{U}(R) := \nabla\mathbf{u}_0 = \Omega\begin{pmatrix} 0 & -1 & 0\\ 1+2Ro & 0 & 0\\ 0 & 0 & 0\end{pmatrix},\\ \mathcal{B}(R) := \nabla\mathbf{B}_0 = \frac{B_\phi^0}{R}\begin{pmatrix} 0 & -1 & 0\\ 1+2Rb & 0 & 0\\ 0 & 0 & 0\end{pmatrix}\end{gathered} \tag{11}$$

the linearized equations of motion take the form

$$\begin{gathered}(\partial_t + \mathcal{U} + \mathbf{u}_0\cdot\nabla)\mathbf{u}' + \frac{1}{\rho}\nabla p' + \frac{1}{\rho\mu_0}\mathbf{B}_0\times(\nabla\times\mathbf{B}') + \frac{1}{\rho\mu_0}\mathbf{B}'\times(\nabla\times\mathbf{B}_0) = \nu\nabla^2\mathbf{u}',\\ (\partial_t - \mathcal{U} + \mathbf{u}_0\cdot\nabla)\mathbf{B}' + (\mathcal{B} - \mathbf{B}_0\cdot\nabla)\mathbf{u}' = \eta\nabla^2\mathbf{B}'.\end{gathered} \tag{12}$$

3. Geometrical optics equations

We seek solutions of the linearized equations (12) in the form of the geometrical optics (or WKB) approximation

$$\begin{aligned}
\mathbf{u}'(\mathbf{x},t,\epsilon) &= \mathrm{e}^{\mathrm{i}\Phi(\mathbf{x},t)/\epsilon}\left(\mathbf{u}^{(0)}(\mathbf{x},t)+\epsilon\mathbf{u}^{(1)}(\mathbf{x},t)\right)+\epsilon\mathbf{u}^{r}(\mathbf{x},t),\\
\mathbf{B}'(\mathbf{x},t,\epsilon) &= \mathrm{e}^{\mathrm{i}\Phi(\mathbf{x},t)/\epsilon}\left(\mathbf{B}^{(0)}(\mathbf{x},t)+\epsilon\mathbf{B}^{(1)}(\mathbf{x},t)\right)+\epsilon\mathbf{B}^{r}(\mathbf{x},t),\\
p'(\mathbf{x},t,\epsilon) &= \mathrm{e}^{\mathrm{i}\Phi(\mathbf{x},t)/\epsilon}\left(p^{(0)}(\mathbf{x},t)+\epsilon p^{(1)}(\mathbf{x},t)\right)+\epsilon p^{r}(\mathbf{x},t),
\end{aligned} \tag{13}$$

where $\mathbf{x}$ is a vector of coordinates, $0<\epsilon\ll 1$ is a small parameter, Φ is a real-valued scalar function that represents the phase of oscillations, $\mathbf{u}^{(j)}$, $\mathbf{B}^{(j)}$ and $p^{(j)}$, $j=0,1,r$ are complex-valued amplitudes, see e.g. Eckhardt and Yao (1995) and Friedlander and Vishik (1995).

Following Landman and Saffman (1987), Dobrokhotov and Shafarevich (1992) and Eckhardt and Yao (1995) we assume further in the text that $\nu=\epsilon^2\tilde{\nu}$ and $\eta=\epsilon^2\tilde{\eta}$ and introduce the derivative along the fluid stream lines

$$\frac{\mathrm{D}}{\mathrm{D}t}:=\partial_t+\mathbf{u}_0\cdot\nabla. \tag{14}$$

Substituting the expansions (13) into equations (12), collecting terms at ϵ^{-1} and ϵ^0, and eliminating the pressure by standard manipulations, we obtain the phase equation

$$\frac{\mathrm{D}\mathbf{k}}{\mathrm{D}t}=-\mathcal{U}^{\mathrm{T}}\mathbf{k}, \tag{15}$$

where $\mathbf{k}=\nabla\Phi$, and the amplitude (or transport) equations

$$\begin{aligned}
\frac{\mathrm{D}\mathbf{u}^{(0)}}{\mathrm{D}t} &= -\left(\mathcal{I}-2\frac{\mathbf{k}\mathbf{k}^{\mathrm{T}}}{|\mathbf{k}|^2}\right)\mathcal{U}\mathbf{u}^{(0)}-\tilde{\nu}|\mathbf{k}|^2\mathbf{u}^{(0)}+\frac{1}{\rho\mu_0}\left(\mathcal{I}-\frac{\mathbf{k}\mathbf{k}^{\mathrm{T}}}{|\mathbf{k}|^2}\right)(\mathcal{B}+\mathbf{B}_0\cdot\nabla)\,\mathbf{B}^{(0)},\\
\frac{\mathrm{D}\mathbf{B}^{(0)}}{\mathrm{D}t} &= \mathcal{U}\mathbf{B}^{(0)}-\tilde{\eta}|\mathbf{k}|^2\mathbf{B}^{(0)}-(\mathcal{B}-\mathbf{B}_0\cdot\nabla)\mathbf{u}^{(0)},
\end{aligned} \tag{16}$$

where $\mathcal{I}$ is a 3×3 identity matrix. In the absence of the magnetic field these equations reduce to those obtained by Landman and Saffman (1987), Dobrokhotov and Shafarevich (1992) and Eckhardt and Yao (1995).

3.1. Amplitude equations

Let the orthogonal unit vectors $\mathbf{e}_R(t)$, $\mathbf{e}_\phi(t)$ and $\mathbf{e}_z(t)$ form a basis in a cylindrical coordinate system moving along the fluid trajectory. With $\mathbf{k}(t)=k_R\mathbf{e}_R(t)+k_\phi\mathbf{e}_\phi(t)+k_z\mathbf{e}_z(t)$, $\mathbf{u}(t)=u_R\mathbf{e}_R(t)+u_\phi\mathbf{e}_\phi(t)+u_z\mathbf{e}_z(t)$, and with the matrix $\mathcal{U}$ from (11), we find that

$$\dot{\mathbf{e}}_R=\Omega(R)\mathbf{e}_\phi,\quad \dot{\mathbf{e}}_\phi=-\Omega(R)\mathbf{e}_R. \tag{17}$$

Hence, the equation (15) in the coordinate form

$$\dot{k}_R-\Omega k_\phi=-\Omega k_\phi-R\partial_R\Omega k_\phi,\quad \dot{k}_\phi+\Omega k_R=\Omega k_R,\quad \dot{k}_z=0$$

yields

$$\dot{k}_R=-R\partial_R\Omega k_\phi,\quad \dot{k}_\phi=0,\quad \dot{k}_z=0. \tag{18}$$

According to Eckhardt and Yao (1995) and Friedlander and Vishik (1995), in order to study physically relevant and potentially unstable modes we have to choose bounded and asymptotically non-decaying solutions of the system (18). These correspond to $k_\phi \equiv 0$ and k_R and k_z being time-independent.

Denoting $\alpha = k_z|\boldsymbol{k}|^{-1}$, where $|\mathbf{k}|^2 = k_R^2 + k_z^2$, we find that $k_R k_z^{-1} = \sqrt{1-\alpha^2}\alpha^{-1}$ and write the partial differential equations (16) for the amplitudes in the coordinate representation. Assuming the solution to the resulting equations in the modal form $\mathrm{e}^{\gamma t + \mathrm{i}m\phi + \mathrm{i}k_z z}$ (Friedlander and Vishik 1995), and taking into account that $B_R^{(0)}k_R + B_z^{(0)}k_z = 0$ in the short-wavelength approximation, we single out the equations for the radial and azimuthal components of the fluid velocity and magnetic field. Introducing the viscous and resistive frequencies as well as the Alfvén frequency of the azimuthal magnetic field

$$\omega_\nu = \widetilde{\nu}|\boldsymbol{k}|^2, \quad \omega_\eta = \widetilde{\eta}|\boldsymbol{k}|^2, \quad \omega_{\mathrm{A}_\phi} = \frac{B_\phi^0}{R\sqrt{\rho\mu_0}} \tag{19}$$

so that

$$Rb = \frac{R}{2\omega_{\mathrm{A}_\phi}}\frac{\partial \omega_{\mathrm{A}_\phi}}{\partial R}, \tag{20}$$

we finally obtain the amplitude equations as follows:

$$\begin{aligned}
&(\gamma + \mathrm{i}m\,\Omega + \omega_\nu)u_R^{(0)} - 2\alpha^2\Omega u_\phi^{(0)} + 2\alpha^2\frac{\omega_{\mathrm{A}_\phi}}{\sqrt{\rho\mu_0}}B_\phi^{(0)} - \frac{\mathrm{i}m\,\omega_{\mathrm{A}_\phi}B_R^{(0)}}{\sqrt{\rho\mu_0}} = 0,\\
&(\gamma + \mathrm{i}m\,\Omega + \omega_\nu)u_\phi^{(0)} + 2\Omega(1+Ro)u_R^{(0)} - \frac{2\omega_{\mathrm{A}_\phi}}{\sqrt{\rho\mu_0}}(1+Rb)B_R^{(0)} - \frac{\mathrm{i}m\,\omega_{\mathrm{A}_\phi}B_\phi^{(0)}}{\sqrt{\rho\mu_0}} = 0,\\
&(\gamma + \mathrm{i}m\,\Omega + \omega_\eta)B_R^{(0)} - \mathrm{i}m\,\omega_{\mathrm{A}_\phi}u_R^{(0)}\sqrt{\rho\mu_0} = 0,\\
&(\gamma + \mathrm{i}m\,\Omega + \omega_\eta)B_\phi^{(0)} - 2\Omega\,Ro\,B_R^{(0)} + 2Rb\,\omega_{\mathrm{A}_\phi}\sqrt{\rho\mu_0}u_R^{(0)} - \mathrm{i}m\,\omega_{\mathrm{A}_\phi}u_\phi^{(0)}\sqrt{\rho\mu_0} = 0.
\end{aligned} \tag{21}$$

3.2. Dimensionless parameters and dispersion relation

The solvability condition for the system (21) yields the dispersion relation

$$\det(\mathbf{M} - \gamma\mathbf{E}) = 0, \tag{22}$$

where $\mathbf{E}$ is the 4×4 identity matrix and

$$\mathbf{M} = \begin{pmatrix}
-\mathrm{i}m\,\Omega - \omega_\nu & 2\alpha^2\Omega & \mathrm{i}\frac{m\omega_{\mathrm{A}_\phi}}{\sqrt{\rho\mu_0}} & -\frac{2\omega_{\mathrm{A}_\phi}\alpha^2}{\sqrt{\rho\mu_0}}\\
-2\Omega(1+Ro) & -\mathrm{i}m\,\Omega - \omega_\nu & \frac{2\omega_{\mathrm{A}_\phi}}{\sqrt{\rho\mu_0}}(1+Rb) & \mathrm{i}\frac{m\omega_{\mathrm{A}_\phi}}{\sqrt{\rho\mu_0}}\\
\mathrm{i}m\,\omega_{\mathrm{A}_\phi}\sqrt{\rho\mu_0} & 0 & -\mathrm{i}m\,\Omega - \omega_\eta & 0\\
-2\omega_{\mathrm{A}_\phi}Rb\sqrt{\rho\mu_0} & \mathrm{i}m\,\omega_{\mathrm{A}_\phi}\sqrt{\rho\mu_0} & 2\Omega\,Ro & -\mathrm{i}m\,\Omega - \omega_\eta
\end{pmatrix}. \tag{23}$$

The polynomial (22) has the same roots as the equation

$$\det(\mathbf{MT} - \gamma\mathbf{ET}) = 0 \tag{24}$$

with $\mathbf{T} = \mathrm{diag}\,(1, 1, (\rho\mu_0)^{-1/2}, (\rho\mu_0)^{-1/2})$.

Now we introduce, in addition to the hydrodynamic (Ro) and magnetic (Rb) Rossby numbers, the magnetic Prandtl number (Pm), the Reynolds (Re) and Hartmann (Ha) numbers, as well as the modified azimuthal wavenumber n:

$$Pm = \frac{\omega_\nu}{\omega_\eta}, \quad Re = \alpha\frac{\Omega}{\omega_\nu}, \quad Ha = \alpha\frac{\omega_{A_\phi}}{\sqrt{\omega_\nu\omega_\eta}}, \quad n = \frac{m}{\alpha}. \tag{25}$$

Dividing equation (24) by Re, we obtain

$$p(\lambda) = \det(\mathbf{H} - \lambda\mathbf{E}) = 0 \tag{26}$$

with $\lambda = \gamma(\alpha\Omega)^{-1}$ and

$$\mathbf{H} = \begin{pmatrix} -\mathrm{i}n - \frac{1}{Re} & 2\alpha & \frac{\mathrm{i}n\,Ha}{\sqrt{Re\,Rm}} & \frac{-2\alpha\,Ha}{\sqrt{Re\,Rm}} \\ -\frac{2(1+Ro)}{\alpha} & -\mathrm{i}n - \frac{1}{Re} & \frac{2Ha(1+Rb)}{\alpha\sqrt{Re\,Rm}} & \frac{\mathrm{i}n\,Ha}{\sqrt{Re\,Rm}} \\ \frac{\mathrm{i}n\,Ha}{\sqrt{Re\,Rm}} & 0 & -\mathrm{i}n - \frac{1}{Rm} & 0 \\ \frac{-2Ha\,Rb}{\alpha\sqrt{Re\,Rm}} & \frac{\mathrm{i}n\,Ha}{\sqrt{Re\,Rm}} & \frac{2Ro}{\alpha} & -\mathrm{i}n - \frac{1}{Rm} \end{pmatrix}, \tag{27}$$

where $Rm = Re\,Pm$ is the magnetic Reynolds number.

3.3. Stability of the Chandrasekhar equipartition solution

Observe that letting

$$Rb = Ro, \quad \Omega = \omega_{A_\phi} \tag{28}$$

in the equation (23) and assuming that $\omega_\nu = 0$ and $\omega_\eta = 0$ we find that the dispersion relation (22) has the following roots:

$$\gamma_{1,2} = 0, \quad \gamma_{3,4} = -2\mathrm{i}\omega_{A_\phi}(m \pm \alpha)$$

which indicates marginal stability.

On the other hand note that $Ha/\sqrt{Re}$ in the matrix (27) is nothing else but the square root of the interaction parameter (or Elsasser number)

$$N := \frac{Ha^2}{Re}. \tag{29}$$

Then, the condition $\Omega = \omega_{A_\phi}$, which is equivalent to

$$Ha = \sqrt{Re\,Rm} \tag{30}$$

is simply

$$N = Rm. \tag{31}$$

With (30), $Rb = Ro$, and $Re \to \infty$ and $Rm \to \infty$ the dispersion relation (26) yields stable solutions in terms of λ

$$\lambda_{1,2} = 0, \quad \lambda_{3,4} = -2\mathrm{i}(n \pm 1).$$

This should not be surprising in view of the fact that at $Rb = Ro = -1$ (28) is nothing else but the well-known Chandrasekhar equipartition solution for the inviscid fluid of infinite electrical conductivity with constant total pressure, see Chandrasekhar (1956, 1961).

Indeed, differentiating the constant total pressure condition $P = \text{const}$, we obtain

$$\frac{\partial p_0}{\partial R} = -\frac{B_\phi^0}{\mu_0}\frac{\partial B_\phi^0}{\partial R}.$$

Substituting this into (6) yields

$$R\Omega^2 = -\frac{B_\phi^0}{\rho\mu_0}\frac{\partial B_\phi^0}{\partial R}$$

which after letting $\Omega = \omega_{\mathrm{A}_\phi}$ transforms into

$$B_\phi^0\left(B_\phi^0 + R\frac{\partial B_\phi^0}{\partial R}\right) = 0.$$

Taking into account that

$$Rb = \frac{1}{2B_\phi^0}\left(R\frac{\partial B_\phi^0}{\partial R} - B_\phi^0\right)$$

we finally get

$$2(B_\phi^0)^2(1 + Rb) = 0.$$

Hence, from the assumption that $\Omega = \omega_{\mathrm{A}_\phi}$ and that the total pressure P is constant, we deduce that $Rb = Ro = -1$. Therefore, the conditions $\Omega = \omega_{\mathrm{A}_\phi}$ and $Rb = Ro = -1$ define the Chandrasekhar (1956) equipartition solution, which is marginally stable, as we have just demonstrated explicitly.

3.4. Michael's criterion and its dissipative extension

By applying the Bilharz stability criterion (Bilharz 1944, Kirillov 2013) to the complex dispersion relation (22) with the matrix (23), we find that for stability against axisymmetric ($m = 0$) perturbations it is necessary and sufficient that

$$Ro > -1 + Rb\frac{\omega_{\mathrm{A}_\phi}^2}{\Omega^2}\frac{\omega_\nu}{\omega_\eta} - \frac{\omega_\nu^2}{4\alpha^2\Omega^2}. \tag{32}$$

Note that the criterion (32) contains the ratio of viscous to resistive frequencies and by this reason the transition to the ideal case is not straightforward: one needs taking first $\omega_\eta = \omega_\nu$ and then letting ω_ν tend to zero. The result is the ideal Michael's criterion

$$Ro > -1 + Rb\frac{\omega_{\mathrm{A}_\phi}^2}{\Omega^2} \tag{33}$$

or, equivalently (Michael 1954, Chandrasekhar 1961)

$$\frac{\mathrm{d}}{\mathrm{d}R}(\Omega^2R^4) - \frac{R^4}{\rho\mu_0}\frac{\mathrm{d}}{\mathrm{d}R}\left(\frac{B_\phi^0}{R}\right)^2 > 0. \tag{34}$$

Putting $\omega_\nu = 0$ in the equation (32) yields

$$Ro > -1, \tag{35}$$

which is Michael's criterion corresponding to the inductionless ($Pm = 0$) and inviscid ($Re \to \infty$) case. In the next section we demonstrate that in the inductionless limit the Michael's criterion can easily be extended so as to comprise both axisymmetric ($m = 0$) and non-axisymmetric ($m \neq 0$) perturbations.

4. Growth rates of AMRI

4.1. Inductionless case ($Pm = 0$)

Taking the definition (29) into account in the dispersion relation (26) and assuming further that the magnetic Prandtl number vanishes, we find the roots of the polynomial $p(\lambda)$ in the following closed form:

$$\lambda = -\mathrm{i}n + N(2Rb - n^2) - \frac{1}{Re} \pm 2\sqrt{(Rb^2+n^2)N^2+\mathrm{i}n(Ro+2)N - 1-Ro}. \tag{36}$$

At small N we can expand λ into the Taylor series

$$\lambda = -\mathrm{i}(n \pm 2\sqrt{1+Ro}) - \frac{1}{Re} + \left(2Rb - n^2 \pm \frac{n(Ro+2)}{\sqrt{Ro+1}}\right) N + O(N^2) \tag{37}$$

evidencing that at $Ro > -1$ it is an inertial wave that will be destabilized by the weak azimuthal magnetic field ($N \ll 1$), no matter how close is its radial profile to the current-free profile $B_\phi \propto R^{-1}$. Destabilization of an inertial wave is characteristic of the inductionless MRI (Kirillov and Stefani 2010, 2011) in contrast to the Tayler instability.

Let λ_r and λ_i denote the real and the imaginary part of the complex root, i.e. $\lambda = \lambda_\mathrm{r} + \mathrm{i}\lambda_\mathrm{i}$. In the inviscid limit when $Re \to \infty$, the equation (36) yields explicit expressions for the growth rates of the perturbation

$$\lambda_\mathrm{r} = N(2Rb - n^2) \pm \sqrt{2[(Rb^2+n^2)N^2 - Ro - 1 + \sqrt{D}]}, \tag{38}$$

where

$$D = N^2n^2((Ro+1)^2+1+N^2(2Rb^2+n^2))+(N^2Rb^2-Ro-1)^2.$$

Putting $\lambda_\mathrm{r} = 0$ in equation (38), we find the condition for marginal stability

$$N = \pm\frac{2\sqrt{-(n^2-4Rb-4)((n^2-2Rb)^2(Ro+1)-(Ro+2)^2n^2)}}{n(n^2-4Rb-4)(n^2-2Rb)} \tag{39}$$

that can be interpreted as a boundary of the instability domain in the N–n plane. The threshold (39) extends the Michael's criterion to arbitrary n in the case when $Pm = 0$ and $Re \to \infty$.

In figure 1 the contour plots of the non-negative growth rates given by equation (38) are shown in projection onto the N–n plane for the special case of Keplerian rotation, i.e. for $Ro = -0.75$. The regions of the non-negative growth rates are bounded by the curves (39). Note that at $n = 0$ we have stability because $Ro = -0.75 > -1$ in accordance with the inductionless Michael's criterion (35) which follows also from (39). Observe that for $Rb < -0.75$ there exist two instability regions, figure 1(a), that touch each other exactly at

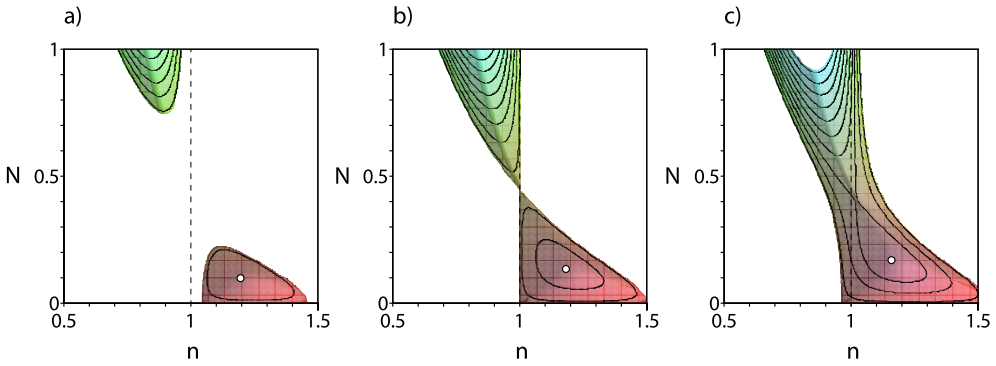

Figure 1. The non-negative growth rates of AMRI in the inductionless ($Pm = 0$) and inviscid ($Re \to \infty$) limit in projection onto the N–n plane at $Ro = -0.75$ and (a) $Rb = -0.76$, (b) $Rb = -0.75$ and (c) $Rb = -0.74$. The open circles mark the maximal growth rates (a) $\lambda_r \approx 0.003$ at $n \approx 1.204$ and $N \approx 0.105$, (b) $\lambda_r \approx 0.005$ at $n \approx 1.180$ and $N \approx 0.139$ and (c) $\lambda_r \approx 0.008$ at $n \approx 1.151$ and $N \approx 0.178$.

$Rb = -0.75$, figure 1(b), and merge into one single region when $Rb > -0.75$, figure 1(c). Remarkably, the intersection point visible in figure 1(b) can be found explicitly if we take $Ro = Rb$ in equation (39). The marginal stability lines intersect then at the point (n, N) with the coordinates

$$n = \pm 2\sqrt{Rb+1}, \quad N = \pm\frac{1}{2}\sqrt{\frac{-(3Rb+2)}{(Rb+1)(Rb+2)}}. \tag{40}$$

For instance, the intersection point in figure 1(b) has the coordinates $n = 1$, $N = \frac{\sqrt{5}}{5}$. In view of the fact that $\alpha \in [0, 1]$ and $n = m/\alpha$, where $m \neq 0$ is an integer, the only physically meaningful unstable region is situated in the domain $|n| \geqslant 1$.

The growth rates reach their maxima inside the physically relevant instability regions in figure 1. The maximal growth rate decreases from $\lambda_r \approx 0.008$ at $Rb = -0.74$ to $\lambda_r \approx 0.003$ at $Rb = -0.76$. With the further decrease in Rb both the size of the lower instability region and the maximal growth rate diminish until at

$$Rb = -\frac{25}{32} = -0.781\,25 \tag{41}$$

the lower instability region shrinks to a point which disappears at smaller Rb.

Indeed, the lower instability region disappears when the roots of the equation (39) become complex. Equivalently,

$$(n^2 - 2Rb)^2(Ro+1) - (Ro+2)^2 n^2 = 0 \tag{42}$$

which factors out into the two equations quadratic in n,

$$n^2 \pm \frac{Ro+2}{\sqrt{Ro+1}} n - 2Rb = 0. \tag{43}$$

The roots n of equations (43) are complex if and only if their discriminant is negative

$$\frac{(Ro+2)^2}{Ro+1} + 8Rb < 0 \tag{44}$$

which yields $Rb < -\frac{25}{32}$ for the Keplerian value of the Rossby number $Ro = -\frac{3}{4}$. On the other hand, the intersection of the marginal stability curves (40) exists at $N \neq 0$ for

$$Ro = Rb < -\frac{2}{3}. \tag{45}$$

At $Ro = Rb = -\frac{2}{3}$ the intersection occurs at $N = 0$, which means that, again, the lower instability region disappears. This effect reminds one of the stability of the Chandrasekhar (1956) equipartition solution for the inviscid fluid of infinite electrical conductivity with constant total pressure. Note, however, that in contrast to Chandrasekhar (1956) we consider here a viscous and resistive fluid in the inductionless limit that is not equivalent to the ideal MHD case as one can see also on the example of Michael's criterion discussed in section 3.4.

4.2. Instability condition

Therefore, when $Ro < -\frac{2}{3}$ and $Rb < Ro$, the instability domain in the N–n plane consists of the two separate regions, see figure 1(a). Since at $-\frac{3}{4} < Rb < -\frac{2}{3}$ and $Rb = Ro$ the parameter n at the intersection is $2\sqrt{Rb+1} > 1$, then according to equation (40) the lower instability region has physical meaning and thus corresponds to the AMRI. This domain of AMRI exists, if

$$Rb \geqslant -\frac{1}{8}\frac{(Ro+2)^2}{Ro+1}. \tag{46}$$

Note that in the case when $Rb = -1$, the condition of existence of AMRI (46) yields $Ro \leqslant 2 - 2\sqrt{2}$, which corresponds to the well-known Liu limit (Liu *et al* 2006, Kirillov and Stefani 2010, Priede 2011, Kirillov *et al* 2012).

Finally, we find the Taylor expansion of the growth rates near $N = 0$

$$\lambda_{\mathrm{r}} = \left(2Rb - n^2 \pm \frac{n(Ro+2)}{\sqrt{Ro+1}}\right)N + \frac{n(Ro+2)(4Rb^2(Ro+1) - n^2Ro^2)}{8(Ro+1)^{5/2}}N^3 + o(N^3). \tag{47}$$

Note that the coefficient in the term that is linear in N is precisely the left hand side of equation (43), which determines the range of unstable values of n at $N = 0$. On the other hand the expansions (37) and (47) explicitly demonstrate that inertial waves can be destabilized in the presence of the azimuthal magnetic field no matter how small is the Elsasser number N. In particular, AMRI of centrifugally stable Keplerian flows can be triggered by an arbitrary weak magnetic field provided that $Rb > -\frac{25}{32}$.

4.3. Finite magnetic Reynolds number

Let us replace in the matrix (27) the ratio $Ha/\sqrt{Re}$ with the $\sqrt{N}$ according to the definition (29) and then let $Re \to \infty$. In the resulting dispersion relation we assume $Ro = Rb$ and apply to it the Bilharz stability criterion (Bilharz 1944, Kirillov 2013). For $Ro = Rb = -0.75$, the Bilharz criterion gives the domain of AMRI presented in figure 2(a). The domain is comprised between the plane $n = 2\sqrt{Rb+1}$ and the surface that intersects the plane along the two straight lines

$$n = 2\sqrt{Rb+1}, \quad N = Rm \pm \frac{1}{2}\sqrt{\frac{-(3Rb+2)}{(Rb+1)(Rb+2)}}. \tag{48}$$

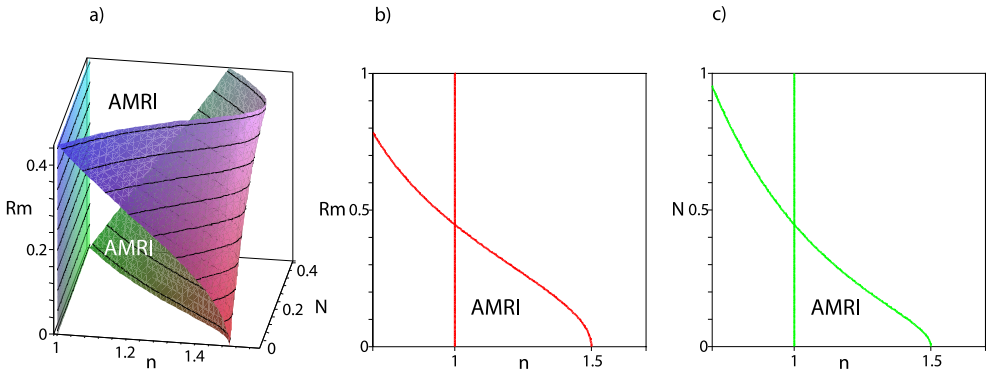

Figure 2. Given $Re \to \infty$ and $Rb = Ro = -0.75$. (a) The domain of AMRI in the (n, N, Rm) space. Its cross-section (b) at $N = 0$ with the intersection at $Rm = \sqrt{5}/5$ and (c) at $Rm = 0$ (inductionless case) with the crossing at $N = \sqrt{5}/5$, cf figure 1(b).

At $N = 0$ and $Rb = -0.75$ the intersection point is at $Rm = \sqrt{5}/5$, see figure 2(b). On the other hand, the intersection point is at $N = \sqrt{5}/5$ when $Rm = 0$ and $Rb = -0.75$, as figure 2(c) demonstrates. Naturally, the cross-section of the domain shown in figure 2(c) exactly coincides with the domain of the inductionless AMRI shown in figure 1(b).

Therefore, we have demonstrated that AMRI of Keplerian flows exists not only in the inductionless limit when $Pm = 0$ or, equivalently, $Rm = 0$, but also at finite values of the magnetic Reynolds number.

5. Conclusions

Using a WKB approach, we have considered the stability condition of a rotating flow under the influence of an azimuthal magnetic field with arbitrary radial dependence. Focusing on the case of small magnetic Prandtl number, we have shown that Keplerian profiles can be destabilized if only the azimuthal field is shallow enough. The necessary induction of $B_\phi(R)$ is comparably small ($Rb \geqslant -0.781\,25$) so that the effect is definitely more on the side of the (inductionless) MRI than on the side of the current-driven Tayler instability with $Rb = 0$ (Seilmayer *et al* 2012).

We have also shown that the point where the hydrodynamic and the magnetic Rossby number are equal plays an essential point for the connectedness of the instability domain. With view on astrophysical applications one has to notice that the shallower than $1/R$ profile of B_ϕ would need some finite magnetic Reynolds number, while the Lundquist number can still be arbitrarily small. Yet, the growth rate would then be rather small, since it is proportional to the interaction parameter. The consequences of our findings for those parts of accretion discs with small magnetic Prandtl numbers are still to be elaborated.

Our results give strong impetus on dedicated MRI experiments in which the magnetic Rossby number can be adjusted by using two independent electrical currents, one through an central, insulated rod, the second one through the liquid metal. A liquid sodium experiment with such a possibility is foreseen in the framework of the DRESDYN project (Stefani *et al* 2012).

Acknowledgments

This work was supported by Helmholtz–Gemeinschaft Deutscher Forschungszentren (HGF) in frame of the Helmholtz Alliance LIMTECH, as well as by Deutsche Forschungsgemeinschaft in frame of the SPP 1488 (PlanetMag).

References

Armitage P J 2011 Dynamics of protoplanetary disks *Annu. Rev. Astron. Astrophys.* **49** 195–236

Balbus S A 2003 Enhanced angular momentum transport in accretion disks *Annu. Rev. Astron. Astrophys.* **41** 555–97

Balbus S A and Henri P 2008 On the magnetic Prandtl number behavior of accretion disks *Astrophys. J.* **674** 408–14

Bilharz H 1944 Bemerkung zu einem Satze von Hurwitz *Z. Angew. Math. Mech.* **24** 77–82

Chandrasekhar S 1956 On the stability of the simplest solution of the equations of hydromagnetics *Proc. Natl Acad. Sci. USA* **42** 273–6

Chandrasekhar S 1960 The stability of non-dissipative Couette flow in hydromagnetics *Proc. Natl Acad. Sci. USA* **46** 137–41

Chandrasekhar S 1961 *Hydrodynamic and Hydromagnetic Stability* (Oxford: Oxford University Press)

Colgate S A *et al* 2011 High magnetic shear gain in a liquid sodium stable Couette flow experiment: a prelude to an $\alpha - \Omega$ synamo *Phys. Rev. Lett.* **106** 175003

Dobrokhotov S and Shafarevich A 1992 Parametrix and the asymptotics of localized solutions of the Navier–Stokes equations in R^3, linearized on a smoothflow *Math. Notes* **51** 47–54

Eckhardt B and Yao D 1995 Local stability analysis along Lagrangian paths *Chaos Solitons Fractals* **5** 2073–88

Friedlander S and Vishik M M 1995 On stability and instability criteria for magnetohydrodynamics *Chaos* **5** 416–23

Herault J, Rincon F, Cossu C, Lesur G, Ogilvie G I and Longaretti P Y 2011 Periodic magnetorotational dynamo action as a prototype of nonlinear magnetic-field generation in shear flows *Phys. Rev.* E **84** 036321

Hollerbach R and Rüdiger G 2005 New type of magnetorotational instability in cylindrical Taylor–Couette flow *Phys. Rev. Lett.* **95** 124501

Hollerbach R, Teeluck V and Rüdiger G 2010 Nonaxisymmetric magnetorotational instabilities in cylindrical Taylor–Couette flow *Phys. Rev. Lett.* **104** 044502

Kirillov O N and Stefani F 2010 On the relation of standard and helical magnetorotational instability *Astrophys. J.* **712** 52

Kirillov O N and Stefani F 2011 Paradoxes of magnetorotational instability and their geometrical resolution *Phys. Rev.* E **84** 036304

Kirillov O N, Stefani F and Fukumoto Y 2012 A unifying picture of helical and azimuthal MRI and the universal significance of the Liu limit *Astrophys. J.* **756** 83

Kirillov O N and Stefani F 2013 Extending the range of the inductionless magnetorotational instability *Phys. Rev. Lett.* **111** 061103

Kirillov O N 2013 *Nonconservative Stability Problems of Modern Physics* (*De Gruyter Studies in Mathematical Physics* vol 14) (Berlin: De Gruyter)

Krueger E R, Gross A and Di Prima R C 1966 On relative importance of Taylor-vortex and non-axisymmetric modes in flow between rotating cylinders *J. Fluid Mech.* **24** 521–38

Landman M J and Saffman P G 1987 The three-dimensional instability of strained vortices in a viscous fluid *Phys. Fluids* **30** 2339–42

Liu W, Goodman J, Herron I and Ji H 2006 Helical magnetorotational instability in magnetized Taylor–Couette flow *Phys. Rev.* E **74** 056302

Michael D H 1954 The stability of an incompressible electrically conducting fluid rotating about an axis when current flows parallel to the axis *Mathematika* **1** 45–50

Petitdemange L, Dormy E and Balbus S A 2008 Magnetostrophic MRI in the earth's outer core *Geophys. Res. Lett.* **35** L15305

Priede J 2011 Inviscid helical magnetorotational instability in cylindrical Taylor–Couette flow *Phys. Rev.* E **84** 066314

Rüdiger G, Gellert M, Schultz M and Hollerbach R 2010 Dissipative Taylor–Couette flows under the influence of helical magnetic fields *Phys. Rev.* E **82** 016319

Rüdiger G, Gellert M, Schultz M, Hollerbach R and Stefani F 2014 The azimuthal magnetorotational instability (AMRI) *Mon. Not. R. Astron. Soc.* **438** 271–7

Seilmayer M, Stefani F, Gundrum T, Weier T, Gerbeth G, Gellert M and Rüdiger G 2012 Experimental evidence for a transient Tayler instability in a cylindrical liquid metal column *Phys. Rev. Lett.* **108** 244501

Stefani F, Gundrum T, Gerbeth G, Rüdiger G, Schultz M, Szklarski J and Hollerbach R 2006 Experimental evidence for magnetorotational instability in a Taylor–Couette flow under the influence of a helical magnetic field *Phys. Rev. Lett.* **97** 184502

Stefani F, Gerbeth G, Gundrum T, Hollerbach R, Priede J, Rüdiger G and Szklarski J 2009 Helical magnetorotational instability in a Taylor–Couette flow with strongly reduced Ekman pumping *Phys. Rev.* E **80** 066303

Stefani F, Eckert S, Gerbeth G, Giesecke A, Gundrum T, Steglich C, Weier T and Wustmann B 2012 DRESDYN—a new facility for MHD experiments with liquid sodium *Magnetohydrodynamics* **48** 103–13

Velikhov E P 1959 Stability of an ideally conducting liquid flowing between cylinders rotating in a magnetic field *Sov. Phys.—JETP—USSR* **9** 995–8